Design of multilayer antireflection coatings made from co-sputtered and low-refractive-index materials by genetic algorithm

Martin F. Schubert[1], Frank W. Mont[1], Sameer Chhajed[1], David J. Poxson[2], Jong Kyu Kim[1], and E. Fred Schubert[1,2,*]

Future Chips Constellation, Rensselaer Polytechnic Institute, Troy, NY 12180 USA
[1]Department of Electrical, Computer, and Systems Engineering, Rensselaer Polytechnic Institute, Troy, NY 12180 USA
[2]Department of Physics, Applied Physics, and Astronomy, Rensselaer Polytechnic Institute, Troy, NY 12180 USA
[*]efschubert@rpi.edu

Abstract: Designs of multilayer antireflection coatings made from co-sputtered and low-refractive-index materials are optimized using a genetic algorithm. Co-sputtered and low-refractive-index materials allow the fine-tuning of refractive index, which is required to achieve optimum anti-reflection characteristics. The algorithm minimizes reflection over a wide range of wavelengths and incident angles, and includes material dispersion. Designs of antireflection coatings for silicon-based image sensors and solar cells, as well as triple-junction GaInP/GaAs/Ge solar cells are presented, and are shown to have significant performance advantages over conventional coatings. Nano-porous low-refractive-index layers are found to comprise generally half of the layers in an optimized antireflection coating, which underscores the importance of nano-porous layers for high-performance broadband and omnidirectional antireflection coatings.

OCIS codes: 310.1210 (Antireflection coatings); 310.4165 (Multilayer design)

References and links

1. W. H. Southwell, "Coating design using very thin high- and low-index layers," Appl. Opt. **24**, 457-460 (1985).
2. J.-Q. Xi, J. K. Kim, and E. F. Schubert, "Silica nanorod-array films with very low refractive indices," Nano Lett. **5**, 1385 (2005).
3. M. F. Schubert, J.-Q. Xi, J. K. Kim, and E. F. Schubert, "Distributed Bragg reflector consisting of high- and low-refractive-index thin film layers made of the same material," Appl. Phys. Lett. **90**, 141115 (2007).
4. J.-Q. Xi, M. F. Schubert, J. K. Kim, M. Chen, S.-Y. Lin, W. Liu, and J. A. Smart, "Optical thin-film materials with low refractive index for broadband elimination of Fresnel reflection," Nature Photon. **1**, 176-179 (2007).
5. W. H. Southwell, "Gradient-index antireflection coatings," Opt. Lett. **8**, 584-583 (1983).
6. D. Poitras and J. A. Dobrowolski, "Toward perfect antireflection coatings: 2. Theory," Appl. Opt. **43**, 1286-1295 (2004).
7. H. Greiner, "Robust optical coating design with evolutionary strategies," Appl. Opt. **35**, 5477-5483 (1996).
8. S. Martin, A. Brunet-Bruneau, and J. Rivory, "Simulated Darwinian evolution of homogeneous multilayer systems: a new method for optical coating design," Opt. Commun. **110**, 503-506 (1994).
9. S. Martin, J. Rivory, and M. Schoenauer, "Synthesis of optical multilayer systems using genetic algorithms," Appl. Opt. **34**, 2247-2254 (1995).
10. J.-M. Yang and C.-Y. Kao, "An evolutionary algorithm for the synthesis of multilayer coatings at oblique light incidence," J. Lightw. Technol. **19**, 559-570 (2001).
11. M. Born and E. Wolf, *Principles of Optics* (Pergamon, Oxford, 1980).
12. H. Nagel, A. G. Aberle, and R. Hezel, "Optimized antireflection coatings for planar silicon solar cells using remote PECVD silicon nitride and porous silicon dioxide," Prog. Photovolt: Res. Appl. **7**, 245-260 (1999).
13. E. Vazsonya, K. De Clercq, R. Einhaus, E. Van Kerschaver, K. Said, J. Poortsmans, J. Szlufcik, and J. Nijs, "Improved anisotropic etching process for industrial texturing of silicon solar cells," Sol. Energy Mater. Sol. Cells **57**, 179-188 (1999).

#92672 - $15.00 USD Received 11 Feb 2008; revised 20 Mar 2008; accepted 27 Mar 2008; published 1 Apr 2008

14. N. H. Karam, R. R. King, M. Haddad, J. H. Ermer, H. Yoon, H. L. Cotal, R. Sudharsanan, J. W. Eldredge, K. Edmondson, D. E. Joslin, D. D. Krut, M. Takahashi, W. Nishikawa, M. Gillanders, J. Granata, P. Hebert, B. T. Cavicchi, and D. R. Lillingron, "Recent developments in high-efficiency $Ga_{0.5}In_{0.5}P$/GaAs/Ge dual- and triple-junction solar cells: steps to next-generation PV cells," Sol. Energy Mater. Sol. Cells **66**, 453-466 (2001).
15. D. J. Friedman and J. M. Olson, "Analysis of Ge junctions for GaInP/GaAs/Ge three-junction solar cells," Prog. Photovolt: Res. Appl. **9**, 179-189 (2001).
16. Z. Q. Li, Y. G. Xiao, and Z. M. Simon Li, "Modeling of multi-junction solar cells by Crosslight APSYS," Proc. SPIE **6339**, 633909 (2006).

1. Introduction

Minimizing optical reflection at dielectric interfaces is a fundamental challenge, and is vital for many applications in optics. It is well known that normal-incidence reflection at a specific wavelength can be minimized using a single layer coating with quarter-wavelength optical thickness and refractive index $n = \sqrt{n_1 n_2}$, where n_1 and n_2 are the refractive indices of the ambient and substrate, respectively. However, a material with the required refractive index may not exist, and additionally, omni-directional and broadband antireflection characteristics are often required for applications such as solar cells or image sensors.

Several methods exist that allow the tuning of refractive index for optical thin films. Alternating layers of a high-index and low-index material, each with thickness much less than the wavelength, produces a film that can be treated as homogenous with refractive index approximated by the volume ratio of the two constituent materials [1]. By changing the relative thickness of each layer, the effective refractive index of the film can be varied between that of the two materials. Oblique-angle deposition can also be used to control the refractive index; in oblique-angle deposition, self-shadowing results in the formation of a nano-porous film of high optical quality [2-4]. The refractive index is related to the porosity of the film, and can be varied by changing the deposition angle. At deposition angles close to 90°, the porosity becomes large and the index decreases to low values. The nano-porous material is termed low-refractive-index (low-*n*) material. Using SiO_2, refractive indices as low as 1.05 have been reported [4]. A third method to create a film with specific refractive index is co-sputtering, in which two materials such as SiO_2 and TiO_2 are simultaneously deposited. The refractive index can be tuned by varying the relative deposition rates of the two materials.

The ability to tune the refractive index is crucial in enabling broadband and omni-directional antireflection coatings. Such coatings generally consist of multilayer stacks in which the refractive index is graded between substrate value and that of air. Using the appropriate refractive index is critical in achieving the best performance. In addition, the inclusion of layers with refractive index close to that of air can greatly reduce reflection, and is impossible using bulk materials [4]. Well-known refractive index profiles for antireflection coatings include the quintic or modified-quintic profiles, which are continuous functions that vary between the substrate refractive index and the index of the ambient material [5,6]. However, these profiles do not give the optimum profile when a finite number of layers is used. Additionally, these profiles require high-refractive-index transparent materials – which often do not exist – to be matched to high-refractive-index substrates, such as silicon. Finally, material dispersion is not considered although it may play a significant role, particularly for broadband applications.

Optimization of multilayer antireflection coatings is difficult because of the high cost of evaluating the performance for a given structure. In addition, the parameter space generally includes many local minima, which makes deterministic optimization schemes that find the local minima unsuitable [7]. To meet these challenges, genetic algorithms have previously been applied in order to optimize a variety of optical coatings [7-10]. Genetic algorithms mirror biological evolution in which the fitness of a population is increased by the processes of selection, crossover, and mutation. In the work presented here, we apply a genetic algorithm to optimize antireflection coatings for silicon image sensors, silicon solar cells, and

#92672 - $15.00 USD Received 11 Feb 2008; revised 20 Mar 2008; accepted 27 Mar 2008; published 1 Apr 2008

triple-junction Ge/GaAs/GaInP solar cells with air as the ambient medium. The calculations consider coatings composed of co-sputtered and low-*n* materials and take material dispersion into account.

2. Numerical approach

Calculations begin with the generation of a population of antireflection coatings with a fixed number of layers whose thicknesses and compositions are randomly generated. A layer may be composed of either nano-porous SiO_2 or any combination of SiO_2/TiO_2, corresponding to low-*n* and co-sputtered films, respectively. The porosity of SiO_2 is limited to 90%, corresponding to a refractive index of 1.05, which has previously been demonstrated [4]. For each member of the population, the largest thicknesses are matched to compositions with the lowest refractive index, and then sorted so that the high-index layers are adjacent to the substrate. This increases the population near the optimum antireflection coating – which is also expected to have monotonically decreasing refractive index and increasing thickness when moving away from the substrate – and reduces the computation time.

After the population has been formed, the fitness of each member is evaluated. The fitness is determined by the reflection coefficient averaged over the wavelength range and angle range of interest, R_{ave}, which is given by,

$$R_{ave} = \frac{1}{\lambda_2 - \lambda_1} \frac{2}{\pi} \int_{\lambda_1}^{\lambda_2} \int_{0}^{\pi/2} \frac{R_{TE}(\lambda,\theta) + R_{TM}(\lambda,\theta)}{2} d\theta \, d\lambda \tag{1}$$

where R_{TE} and R_{TM} are the TE and TM reflection coefficients. In practice, the fitness function may easily be modified to give greater weight to certain angles of incidence or to certain wavelengths to take into account the responsivity of a particular solar cell, the solar spectrum, or the orientation of a solar cell with respect to the sun, in order to maximize the power produced by a solar cell, for example. The fittest member of the population is the one with lowest average reflection coefficient. The method for calculating the reflection coefficients of a multilayer stack was described by Born and Wolf [11]. The population is sorted by fitness, and a percentage of the worst members are then discarded. These are replaced by the offspring of two other antireflection coatings, which are selected at random from the remaining members of the population. Offspring antireflection coatings are generated by a process of crossover and mutation. In crossover, a set of layers for the new offspring is taken from one parent, and the remainder is taken from the second parent. In mutation, the composition and thickness of each layer is given a random perturbation. Once the worst members of the population have been replaced by new offspring, the fitness of each is evaluated, and the process repeats until good convergence is achieved. Finally, using a deterministic algorithm, the local minima near the fittest member of the population is found.

3. Silicon image sensor

Silicon image sensors are widespread in digital cameras, and generally capture light in the visible wavelength range. Low reflection from the sensor surface is desirable to increase the absorbed light and decrease the noise in the resultant image. The reflection coefficient should also be low over a wide range of incident angles; depending upon lens configuration, the angle of incidence of light on the sensor surface can vary. Strong angular dependence of reflection can produce undesirable vignetting. Finally, the reflection coefficient must be consistently low across the entire visible wavelength range of 400 to 700 nm.

Figure 1 shows the reflection coefficient of bare silicon and optimized one- and three-layer antireflection coatings as a function of wavelength and incident angle. The reflection for bare silicon is high throughout the range of wavelengths and angles. The single-layer coating has a minimum near λ = 540 nm at small angles of incidence, where the reflection coefficient is

#92672 - $15.00 USD Received 11 Feb 2008; revised 20 Mar 2008; accepted 27 Mar 2008; published 1 Apr 2008

below 0.5%, and reduced reflection coefficient values throughout the range compared to bare silicon. The three-layer coating has three distinct minima which combine to give reflection coefficients less than 2% for the majority of wavelengths and incident angles; for optimized antireflection coatings for the silicon image sensor, the number of local minima in reflection is equal to the number of layers used. The layer compositions and thicknesses of these optimized coatings are listed in Table 1. Layer thicknesses and compositions should be within several percent of the specified values in order to achieve performance similar to the given structure. In the optimized antireflection structures for the silicon image sensor, generally about half of the layers are composed of nano-porous low-*n* SiO_2. The same is true for antireflection coatings optimized for other applications, as will be shown later. This finding underscores the importance of low-*n* materials in achieving high performance antireflection coatings.

The reflection coefficient as a function of layer number for optimized coatings is shown in Fig. 2. The reflection coefficient initially decreases rapidly as more layers are added, and then becomes almost constant. The angle- and wavelength-averaged reflectivity of the three- and four-layer antireflection coatings are similar at 4.4% and 3.9%, respectively; the top layers of the three- and four-layer antireflection coatings each are composed of 90% porous SiO_2 – which gives the lowest allowed refractive index, while the bottom layers of both coatings are pure or nearly-pure TiO_2 – which gives the highest achievable refractive index. As mentioned above, the three- and four-layer coatings also have similar reflection coefficients. This is a general characteristic for antireflection coatings: once a sufficient number of layers is used so that the optimum stack contains layers with both the highest and lowest allowed refractive index, increasing the layer number further has only a small effect on the reflection coefficient.

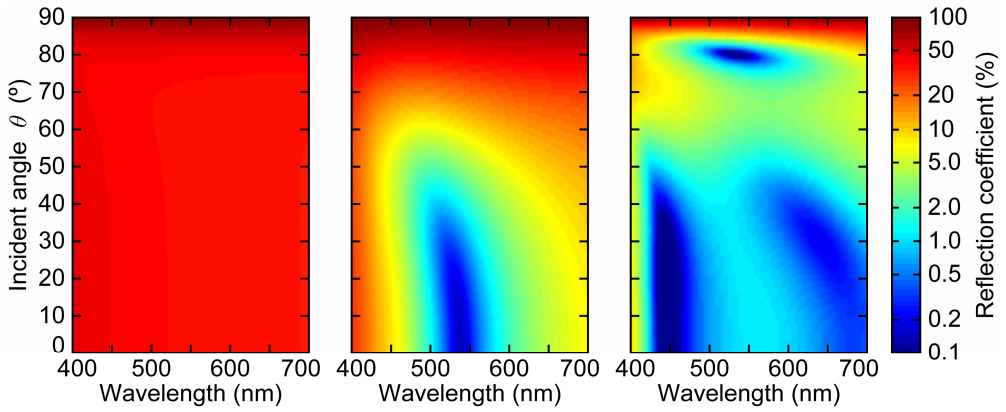

Fig. 1. Reflection coefficient of (left) silicon and optimized (center) one- and (right) three-layer antireflection coatings for silicon image sensors versus wavelength and incident angle.

Table 1. Thickness *t* (in nm) and composition *c* of individual layers for optimized silicon image sensor antireflection coatings. (CS = co-sputtered layer, NP = nano-porous low-*n* layer)

	1-layer	**2-layer**	**3-layer**	**4-layer**
t_1	68.4	327.7	362.8	293.4
t_2	-	65.6	91.9	115.6
t_3	-	-	42.7	75.4
t_4	-	-	-	41.7
c_1	CS, 36% TiO_2	NP, 14% SiO_2	NP, 10% SiO_2	NP, 10% SiO_2
c_2	-	CS, 42% TiO_2	CS, 4% TiO_2	NP, 35% SiO_2
c_3	-	-	CS, 98% TiO_2	CS, 15% TiO_2
c_4	-	-	-	CS, 100% TiO_2

#92672 - $15.00 USD Received 11 Feb 2008; revised 20 Mar 2008; accepted 27 Mar 2008; published 1 Apr 2008

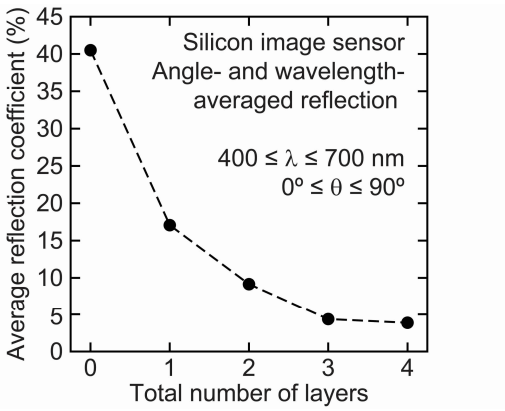

Fig. 2. Angle- and wavelength-averaged reflection coefficient as a function of the number of layers for optimized antireflection coatings for a silicon image sensor.

4. Silicon solar cell

The silicon solar cell is one of the most widespread technologies for photovoltaics; the relevant spectral range for this application is 400 to 1100 nm. One or two-layer antireflection coatings and surface texturing are common methods used to reduce reflection from the surface and increase efficiency [12,13]. Using the genetic algorithm approach, antireflection coatings for silicon solar cells with up to five layers are optimized. The reflection coefficient as a function of wavelength and incident angle is shown in Fig. 3 for optimized one-, two-, and four-layer antireflection coatings. As before, the number of minima in reflection is equal to the number of layers in the antireflection coating. The compositions of optimized coatings are shown in Table 2. Again, nano-porous layers compose roughly half of the layers in an antireflection coating with a given number of layers.

Compared to the one- and two-layer coatings, the four-layer coating yields substantially reduced reflection, particularly at the largest incident angles and shortest wavelengths. Note that the one- and two-layer coatings feature one co-sputtered layer and both nano-porous low-*n* and co-sputtered layers, respectively, which will give enhanced performance compared to conventional one- and two-layer coatings. The angle- and wavelength-averaged reflection

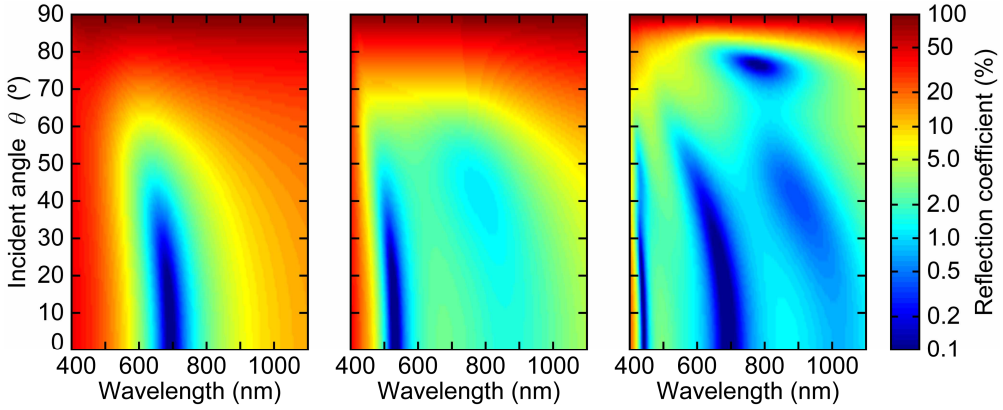

Fig. 3. Reflection coefficient of (left) one-, (center) two-, and (right) four-layer antireflection coatings optimized for silicon solar cells versus wavelength and incident angle.

#92672 - $15.00 USD Received 11 Feb 2008; revised 20 Mar 2008; accepted 27 Mar 2008; published 1 Apr 2008

Table 2. Thickness *t* (in nm) and composition *c* of individual layers for optimized silicon solar cell antireflection coatings. (CS = co-sputtered layer, NP = nano-porous low-*n* layer)

	1-layer	**2-layer**	**3-layer**	**4-layer**	**5-layer**
t_1	91.2	133.1	432.8	432.6	388.7
t_2	-	64.0	113.3	145.8	159.3
t_3	-	-	58.6	79.7	107.8
t_4	-	-	-	51.2	70.1
t_5	-	-	-	-	50.5
c_1	CS, 36% TiO_2	NP, 78% SiO_2	NP, 11% SiO_2	NP, 10% SiO_2	NP, 10% SiO_2
c_2	-	CS, 70% TiO_2	CS, 3% TiO_2	NP, 54% SiO_2	NP, 29% SiO_2
c_3	-	-	CS, 82% TiO_2	CS, 28% TiO_2	NP, 81% SiO_2
c_4	-	-	-	CS, 100% TiO_2	CS, 37% TiO_2
c_5	-	-	-	-	CS, 100% TiO_2

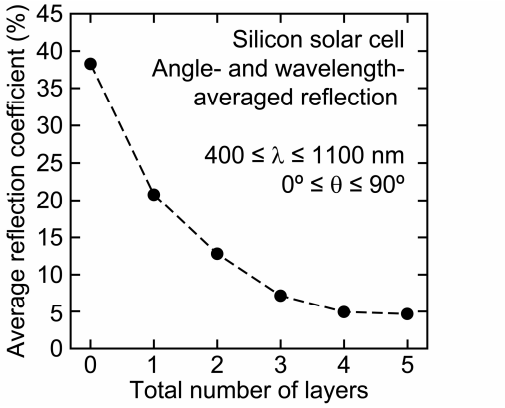

Fig. 4. Angle- and wavelength-averaged reflection coefficient as a function of the number of layers for optimized antireflection coatings for silicon solar cells.

coefficients are plotted in Fig. 4 as a function of the number of layers. As discussed above, when an optimized antireflection coating includes layers with both the lowest allowed and highest allowed refractive index, adding additional layers generally provides little benefit. In the case of the silicon solar cell, which is identical to the image sensor with the exception that the relevant wavelength range is broader, a larger number of layers is needed to reach this threshold. In the image sensor, going from three to four layers reduces average reflectivity by 11.1%, while for the solar cell, reflectivity is reduced by 31.1%. Adding an fifth layer to the solar cell antireflection coating reduces reflection by an additional 5.6%.

5. GaInP/GaAs/Ge triple-junction solar cell

Multi-junction solar cells have achieved the highest efficiency of any photovoltaic technology available [14-16]. Because of the higher cost associated with fabrication, a primary intended use is in concentrator systems, where lenses or reflectors are used to collect sunlight over a large area and focus it on a small active area where the solar cell is located. Because of the nature of concentrator systems, generally there is always some light incident upon the solar cell at oblique angles, which makes broadband and omni-directional antireflection coatings especially important in this application.

The structure used in calculations consists of a GaInP/GaAs/Ge stack with thicknesses as given in [16]. The bottom germanium layer is assumed to be infinitely thick. The structure in [16] also includes intermediate layers which act as tunnel junctions or back surface field structures; however, the refractive indices of materials used in some of these layers are not well reported. Therefore, the triple-junction solar cell is treated as a simple three-layer stack,

#92672 - $15.00 USD Received 11 Feb 2008; revised 20 Mar 2008; accepted 27 Mar 2008; published 1 Apr 2008

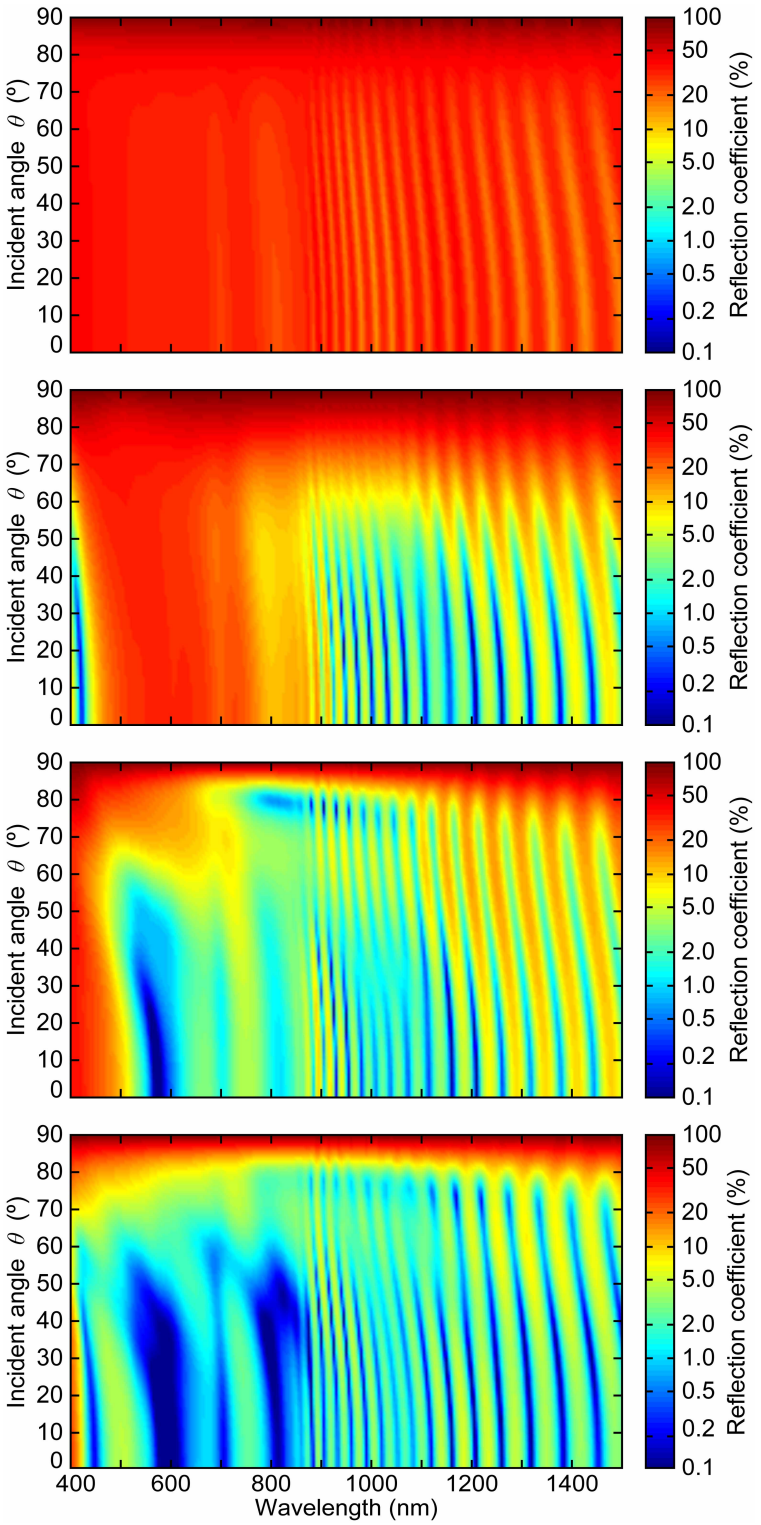

Fig. 5. Reflectivity of (top to bottom) a bare GaInP/GaAs/Ge triple-junction solar cell, and triple-junction solar cells with optimized one-, three-, and five-layer antireflection coatings.

#92672 - $15.00 USD Received 11 Feb 2008; revised 20 Mar 2008; accepted 27 Mar 2008; published 1 Apr 2008

Table 3. Thickness t (in nm) and composition c of individual layers for optimized GaInP/GaAs/Ge triple-junction solar cell antireflection coatings. (CS = co-sputtered layer, NP = nano-porous low-n layer)

	1-layer	**2-layer**	**3-layer**	**4-layer**	**5-layer**	**6-layer**
t_1	162.7	294.9	544.4	550.9	525.0	489.8
t_2	-	132.0	137.5	168.1	195.8	206.5
t_3	-	-	78.3	94.0	108.9	127.7
t_4	-	-	-	63.0	74.1	90.1
t_5	-	-	-	-	53.2	66.5
t_6	-	-	-	-	-	52.2
c_1	CS, 27% TiO_2	NP, 36% SiO_2	NP, 11% SiO_2	NP, 10% SiO_2	NP, 10% SiO_2	NP, 10% SiO_2
c_2	-	CS, 44% TiO_2	CS, 0% TiO_2	NP, 58% SiO_2	NP, 39% SiO_2	NP, 28% SiO_2
c_3	-	-	CS, 61% TiO_2	CS, 25% TiO_2	CS, 5% TiO_2	NP, 69% SiO_2
c_4	-	-	-	CS, 82% TiO_2	CS, 48% TiO_2	CS, 17% TiO_2
c_5	-	-	-	-	CS, 100% TiO_2	CS, 57% TiO_2
c_6	-	-	-	-	-	CS, 100% TiO_2

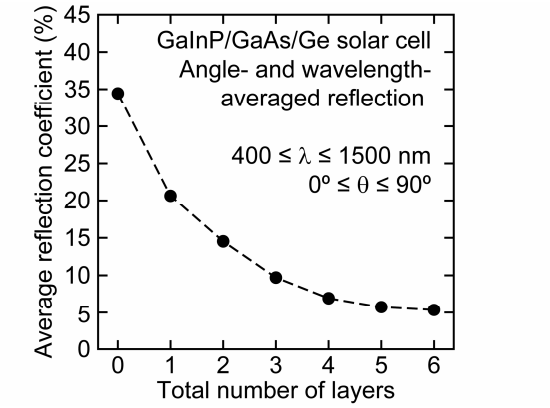

Fig. 6. Angle- and wavelength-averaged reflection coefficient as a function of the number of layers for optimized antireflection coatings for GaInP/GaAs/Ge triple-junction solar cells.

although in principle any number of layers could be included in the calculation. The wavelength range considered in for the antireflection coatings is 400 nm to 1500 nm. Table 3 shows the composition and thickness of each layer for optimized antireflection coatings with up to six layers. Figure 5 shows the reflectivity as a function of angle for the bare triple-junction solar cell, as well as the solar cell with optimized one-, three-, and five-layer antireflection coatings.

For each case shown in Fig. 5, the reflectivity at wavelengths longer than 700 nm, and particularly longer than 900 nm shows pronounced fringing. These longer wavelengths pass through the top junction or both the top and middle junctions of the solar cell without being absorbed; interference of light within these layers produces the reflectivity fringes. When a single-layer antireflection coating is added, reflectivity is initially reduced at longer wavelengths. As more layers are added, reflectivity across the entire range of wavelengths and incident angles is reduced. Figure 6 plots the reflectivity of the optimized antireflection coatings as a function of total number of layers.

6. Conclusion

We have described a method for optimizing antireflection coatings made of co-sputtered and nano-porous low-refractive-index coatings. The method is based on a genetic algorithm which is well suited for the task of optimizing optical thin-film coatings, given the fact that the design space of multi-layered optical coatings includes many local minima of the fitness function, i.e., the average reflectivity. The optimization method was applied to silicon image

#92672 - $15.00 USD Received 11 Feb 2008; revised 20 Mar 2008; accepted 27 Mar 2008; published 1 Apr 2008

sensors and solar cells, as well as a triple-junction GaInP/GaAs/Ge solar cell. In each case, nano-porous layers constitute roughly half of the total number of layers in optimized antireflection coatings, which underscores the importance of low-refractive-index materials for high-performance antireflection coatings.

Acknowledgments

The authors gratefully acknowledge support by the National Science Foundation, the Department of Energy, Sandia National Laboratories, New York State, Samsung Electro-Mechanics Company, Crystal IS Corporation, and Troy Research Corporation.

#92672 - $15.00 USD Received 11 Feb 2008; revised 20 Mar 2008; accepted 27 Mar 2008; published 1 Apr 2008